








Original Research

Inhibition of Endothelial–Mesenchymal Transition Mediated by Activin Receptor Type IIA Attenuates Valvular Injury Induced by Group A Streptococcus in Lewis Rats

Zirong Lu^{1,2,3,†} , Yuan Li^{1,2,3,†} , Chuanghong Lu^{1,2,3} , Zhongyuan Meng^{1,2,3} ,
Ling Bai^{1,2,3} , Feng Huang^{1,2,3,*} , Zhiyu Zeng^{1,2,3,*} 

¹Department of Cardiology, The First Affiliated Hospital of Guangxi Medical University, 530021 Nanning, Guangxi, China

²Guangxi Key Laboratory of Precision Medicine in Cardio-cerebrovascular Diseases Control and Prevention, 530021 Nanning, Guangxi, China

³Guangxi Clinical Research Center for Cardio-cerebrovascular Diseases, 530021 Nanning, Guangxi, China

*Correspondence: huangfeng@stu.gxmu.edu.cn (Feng Huang); zengzhiyu@gxmu.edu.cn (Zhiyu Zeng)

†These authors contributed equally.

Academic Editor: Ioanna-Katerina Aggeli

Submitted: 31 August 2024 Revised: 4 October 2024 Accepted: 11 November 2024 Published: 7 January 2025

Abstract

Background: Rheumatic heart disease (RHD), which is caused mainly by Group A Streptococcus, leads to fibrotic damage to heart valves. Recently, endothelial–mesenchymal transition (EndMT), in which activin plays an important role, has been shown to be an important factor in RHD valvular injury. However, the mechanism of activin activity and EndMT in RHD valvular injury is not clear. **Methods:** Our study was divided into two parts: *in vivo* and *in vitro*. We constructed a small interfering RNA (ACVR2A-siRNA) by silencing activin receptor type IIA (ACVR2A) and an adeno-associated virus (AAV-ACVR2A) containing a sequence that silenced ACVR2A. The EndMT cell model was established via human umbilical vein endothelial cells (HUVECs), and the RHD animal model was established via female Lewis rats. ACVR2A-siRNA and AAV-ACVR2A were used in the above experiments. **Results:** EndMT occurred in the valvular tissues of RHD rats, and activin and its associated intranuclear transcription factors were also activated during this process, with inflammatory infiltration and fibrotic damage also occurring in the valvular tissues. After inhibition of ACVR2A, EndMT in valvular tissues was also inhibited, and inflammatory infiltration and fibrosis were reduced. Endothelial cell experiments suggested that mesenchymal transition could be stimulated by activin and that inhibition of ACVR2A attenuated mesenchymal transition. **Conclusions:** Activin plays an important role in signal transduction during EndMT after activation, and inhibition of ACVR2A may attenuate RHD valvular damage by mediating EndMT. Targeting ACVR2A may be a therapeutic strategy to alleviate RHD valvular injury.

Keywords: activin; ACVR2A; rheumatic heart disease; endothelial–mesenchymal transition; valvular injury

1. Introduction

Rheumatic heart disease (RHD) is an immune-mediated disease triggered by group A streptococcal (GAS) bacteria [1]. Although the worldwide prevalence of RHD has decreased in low- and middle-income countries, this disease remains a major public health challenge, predominantly affecting younger people, including children, teenagers, and young adults, in these regions [2,3]. Globally, the number of RHD patients has surpassed a quarter of the total number of cancer patients, and according to relevant data, the number of RHD-related deaths is as high as 250,000 annually [4]. RHD typically results in damage to valves, and almost all cases of heart valvular damage caused by RHD involve the mitral valve [5]. The pathogenic mechanism of RHD and methods for preventing and treating RHD have not been fully elucidated in the last decade of research [6]. Patients with rheumatic mitral valvular dysfunction may undergo surgical repair [7]. However, the adverse effects and complications associated with valvular surgery are far-reaching [8]. Thus, the identification of

novel therapeutic approaches and related targets for treating RHD valvular injury is urgently needed.

The mitral valve consists of two layers of endothelial cells closely covering connective tissue. If the mitral valve is damaged, the endothelial cells become irritated and inflamed, and when the connective tissue is involved, a fibrotic scar can form that is directly associated with valvular disease [9]. Endothelial–mesenchymal transition (EndMT), which is linked to endothelial damage, involves the transformation of endothelial cells from their characteristic state (expressing vascular endothelial (VE)-cadherin and platelet endothelial cell adhesion molecule-1 (PECAM-1/CD31)) to a mesenchymal phenotype (expressing α -smooth muscle actin (α -SMA) and vimentin) [10,11]. EndMT is necessary for normal heart valvular development. However, under pathological conditions, this process can lead to valvular dysfunction and promote the development of cardiac valvular fibrosis [12,13]. EndMT begins in response to external signals and is usually initiated by transforming growth factor- β (TGF- β) [14], which has been shown to be a potent inducer of EndMT [15]. The



TGF- β pathway is important for regulating EndMT, and the key factors involved in this pathway are activin, Smad family member 2 (Smad2) and Smad3 [16]. Endothelial cell damage can be effectively reduced by inhibiting the pathways associated with the initiation of EndMT [17,18].

Activin belongs to the TGF- β subfamily and has a similar mode of expression to that of TGF- β during signal transduction [19]. During signaling in cells, activin and activin receptor type II (ACVR2) form a complex at the cell membrane before binding to activin receptor type I (ACVR1) as the ACVR2-activin-ACVR1 complex. The complex then becomes a loading station for Smad2/3 [20, 21]. Smad2/3 undergo phosphorylation at the Ser residue of the C-terminal structural domain and bind to Smad4 [22–24]. Upon penetration into the cell nucleus, the Smad component triggers the activation of intranuclear transcription factors linked to EndMT, including lymphoid enhancer factor-1 (LEF-1), snail family transcriptional repressor 1 (Snail1), transcription factor twist family basic helix-loop-helix (bHLH) transcription factor 1 (TWIST), zinc finger E-box-binding homeobox (ZEB) 1 and ZEB2 [25–29]. Previous research has indicated that the phosphorylation of Smad2 and Smad3 is important in the EndMT process, which regulates cardiac fibrosis [30,31]. Furthermore, a recent investigation revealed that both the activin/Smad2/3 pathway and EndMT are associated with RHD valvular injury [32]. However, these studies did not elucidate the mechanism underlying the interaction between activin and EndMT in RHD valvular injury.

Activin is able to bind strongly to activin receptor type II, which includes activin receptor type IIA (ACVR2A) and activin receptor type IIB (ACVR2B) [33]. In recent years, ACVR2A has received much attention in the study of antifibrosis and mesenchymal transition [34,35]. To gain insight into the relevance and mechanism of action of activin and EndMT in RHD valvular injury, the present study was conducted *in vivo* and *in vitro* by silencing ACVR2A. In our *in vitro* study, we chose human umbilical vein endothelial cells (HUVECs) as our study subjects, and we evaluated the role of activin in the mesenchymal transition of HUVECs via the use of recombinant proteins. Moreover, we constructed a small interfering RNA (ACVR2A-siRNA) that silenced ACVR2A and applied it to a cell model of EndMT to explore its effect. In our *in vivo* studies, we constructed an adeno-associated virus (AAV-siACVR2A) loaded with silenced ACVR2A sequences, applied it to an animal model of RHD established in female Lewis rats, and explored the role of AAV-siACVR2A by evaluating the valvular organization of the animal model.

This study contributes to the understanding of the specific pathogenic mechanisms of RHD valvular injury and provides a useful reference for the prevention and treatment of RHD valvular injury.

2. Materials and Methods

2.1 Preparation of Antigen

Group A Streptococcus (GAS, American Type Culture Collection) was grown in brain-heart culture medium (024053, Guangdong Huankai Microbial Technology Co., Ltd., Guangdong, China) at a steady temperature of 37 °C. After 24 hours, the GAS bacteria were rinsed with normal saline (NS) and then inactivated by immersion in 4% paraformaldehyde (P1110, Beijing Solarbio Science & Technology Co., Ltd., Beijing, China). After inactivation, the GAS bacteria were rinsed and placed in NS at a concentration of 4.0×10^{11} CFU/mL [36]. The GAS bacteria were emulsified at the time of administration via a sonicator (VCX130, Sonics & Materials, Inc, Newtown, CT, USA).

2.2 Experimental Animals

Twenty-four healthy female Lewis rats, aged 10 weeks, were obtained from Beijing Viton Lihua Laboratory Animal Technology Co., Ltd. (Beijing, China). The rats weighed between 160 and 180 g. The rats were kept in a laboratory at Guangxi Medical University's Animal Experiment Center, which is a specific pathogen-free (SPF) room. The temperature was maintained at 23 ± 2 °C, with a 12-hour cycle alternating between light and darkness. Prior to the start of the experiment, the rats were allowed to acclimate to the novel environment for one week. The rats were granted unrestricted mobility within their enclosures and were supplied with adequate drinking water and standardized rat chow. The research followed ethical standards for the care and use of laboratory animals. This study was approved by the Ethics Committee of the First Affiliated Hospital of Guangxi Medical University (Approval Number: 202209145).

2.3 In Vivo Gene Therapy

The experimental rats were pretreated with a recombinant adeno-associated virus (AAV) vector (AAV-siACVR2A; Hanheng Biotechnology (Shanghai) Co., Ltd., Shanghai, China) carrying the ACVR2A-siRNA sequence. To analyze the possible effects of the AAV vector on the rats, a negative control group (AAV-control group) was also established in which the rats were pretreated with AAV without the target sequence. The siRNA sequence of the ACVR2A target gene was 5'-GGAAGTTGTTGTGCATAAA-3'. The ACVR2A target gene shRNA sequences were as follows: top strand, 5'-AATTCGGAAGTTGTTGTGCATAAACTCGAGTTTATG CACAACAACCTCCTTTTTTTG-3'; and bottom strand, 5'-GATCCAAAAGGAAGTTGTTGTGCATAAACTCGAGT TTATGCACAACAACCTCCG-3'.

2.4 Groups and Treatments

The rats were arbitrarily grouped into four groups (6 rats/group): the control group, RHD group, RHD+AAV-control group (hereinafter referred to as the AAV-control

group) and RHD+AAV-siACVR2A group (hereinafter referred to as the AAV-siACVR2A group). The RHD experimental model was constructed over 8 weeks via an approach described in prior investigations [37,38]. First, a combination of GAS (4.0×10^{11} CFU/mL) and complete Freund's adjuvant (F5881, Sigma–Aldrich, Darmstadt, Germany) was made by mixing them at a 1:1 ratio. Then, 100 μ L of this mixture was injected into the hind paw pad of each rat under gas anesthesia at a 2% isoflurane (R510-22-10, RWD Life Science Co., Ltd., Shenzhen, China) concentration. After waiting for one week, 500 μ L of the above mixture was administered into the abdomen of the rats, and this mixture was maintained for 4 weeks once a week. During the remaining weeks, 4.0×10^{11} CFU/mL GAS was injected subcutaneously into the abdominal cavity of the rats at a dose of 500 μ L once a week. Before the experiment, rats in the AAV-control and AAV-siACVR2A groups were injected individually with a single dose of 2.5×10^{11} viral particles diluted with 200 μ L of NS via the tail vein, and after 3 weeks, these rats underwent the same injection procedure for modeling. The control rats were subjected to the same protocol as the model rats were, but the injection medium used was NS. The euthanasia endpoint was defined as a reduction of more than 15% of the animal's weight, together with a decrease in feeding and drinking. In this study, no rat reached this endpoint. At the end of all dosing periods, the rats were euthanized via the intraperitoneal administration of pentobarbital sodium (P3761, Sigma–Aldrich, Darmstadt, Germany) at a concentration of 150 mg/kg to collect the heart valves.

2.5 Sample Preparation

The mitral valve specimens from dead rat hearts were collected in a timely manner, rapidly transferred to liquid nitrogen, and then stored at -80°C for additional experimental analysis.

2.6 Histochemical Analysis

After incubation in 4% paraformaldehyde for 12 hours, the tissue blocks were dehydrated through a range of ethanol concentrations. Afterward, the tissue blocks were promptly transferred into molten paraffin to maintain the temperature and subsequently embedded once the paraffin fully enveloped the tissue blocks. Each block was sequentially sliced into 5 μ m thick sections for hematoxylin and eosin (H&E) staining and Sirius red staining. The H&E staining process involved immersing the samples in a hematoxylin solution at ambient temperature for 4–10 minutes, followed by 2–3 minutes of immersion in an eosin staining solution containing alcohol. H&E staining kits (G1005) were purchased from Wuhan Servicebio Technology Co., Ltd (Wuhan, China). A BX43 light microscope (BX43, Olympus Corporation, Tokyo, Japan) was used to record the results. The Sirius red staining process involved the use of Sirius red staining solution (MM1036, Shanghai Maokang

Biotechnology Co., Ltd., Shanghai, China) at ambient temperature for one hour. Polarized light pictures were then captured with a BX43 confocal microscope (BX43, Olympus Corporation, Tokyo, Japan).

2.7 Immunohistochemistry

Immunohistochemical analysis was conducted via the use of purified polyclonal antibodies against rat CD31, α -SMA, collagen type I alpha 1 (COL1A1) and vimentin. Paraffin sections (5 μ m thick) were treated with a 3% aqueous solution of hydrogen peroxide at ambient temperature and maintained in darkness for 25 minutes. The sections were subsequently blocked with 3% bovine serum albumin (GC305006, Servicebio) under ambient conditions for 30 minutes. Subsequently, the samples were incubated with primary antibodies for 12 hours. The samples were then incubated with a horseradish peroxidase (HRP)-conjugated anti-rabbit secondary antibody (1:200, G1213, Servicebio) for 50 minutes at room temperature. The results were recorded with a BX43 microscope.

2.8 Cell Culture

HUVECs (Shanghai Zhong Qiao Xin Zhou Biotechnology Co., Ltd., Shanghai, China) were grown in endothelial cell medium (ECM, 1001, ScienCell Research Laboratories, Carlsbad, CA, USA) at 37°C and 5% CO_2 . HUVECs were stimulated with 10 ng/mL recombinant human TGF- β 1 (HZ-1011, Proteintech Group, Inc., Wuhan, China) or 10 ng/mL recombinant human activin A (APA001Hu01, Cloud-Clone Corp, Wuhan, China) for 48 hours. TGF- β 1 at a concentration of 10 ng/mL successfully induces EndMT in HUVECs, as demonstrated in previous studies [39–41]. Therefore, TGF- β 1 was used as a positive control. To investigate the role of activin A in endothelial cell mesenchymal transition, we first transfected endothelial cells with ACVR2A-siRNA and subsequently treated endothelial cells with activin A. All cell lines were validated by short tandem repeat profiling and tested negative for mycoplasma.

2.9 siRNA Transfection

Hanheng Biotechnology (Shanghai) Co., Ltd. (Shanghai, China). provided the siRNAs. HUVECs were transfected with siRNAs via Lipofectamine 3000 (L3000015, Thermo Fisher Scientific, Inc., Waltham, MA, USA). Two microliters of siRNA and 5 μ L of Lipofectamine 3000 transfection reagent were added to 250 μ L of Opti-MEM (31985070, Thermo Fisher Scientific) solution, mixed separately, and left to stand to form the siRNA-Lipofectamine 3000 complex. The complex was used to treat HUVECs. The ACVR2A-siRNA used were as follows: forward, 5'-GGAAGUUGUUGUGCAUAAATT-3' and reverse, 5'-UUUAUGCACAACAACUUCCTT-3'. The negative control (NC)-siRNA used were as follows: forward, 5'-UUCUCCGAACGUGUCACGUTT-3' and reverse, 5'-ACGUGACACGUUCGGAGAATT-3'.

2.10 Reverse Transcription Quantitative Polymerase Chain Reaction

TRIzol® reagent (15596026CN, Thermo Fisher Scientific, Inc., Waltham, MA, USA) was used to extract total RNA from heart valves or cultured HUVECs. The RNA was converted into cDNA via a reagent kit (YFXM0009, YIFEIXUE Biotech. Co., Ltd., Nanjing, China). RT-qPCR was conducted with 2× SYBR Green Fast qPCR Master Mix (YFXM0001, YIFEIXUE Biotech. Co., Ltd., Nanjing, China) on a real-time PCR system (Bio-Rad). The results were normalized to the relative expression of each target gene via the $2^{-\Delta\Delta C_t}$ method, and either glyceraldehyde-3-phosphate dehydrogenase (*GAPDH*) or β -actin was used as the reference gene. Table 1 summarized the primer sequences used in this study.

2.11 Western Blotting

PMSF (P0100, Solarbio Science & Technology Co., Ltd., Beijing, China), protein phosphatase inhibitor (P1260, Solarbio), and RIPA buffer (R0010, Solarbio) were made into a cell lysate with a ratio of 1:1:100. Valve tissues or cells were lysed for a period of 1 hour. Protein concentration was determined by BCA assay and individual samples contained 30 mg of protein. Then electrophoresis on 7.5–12.5% sodium dodecyl sulfate (SDS)/polyacrylamide gel electrophoresis (PAGE) gels, followed by transfer to polyvinylidene fluoride (PVDF) membranes (ISEQ00005, EMD Millipore, Darmstadt, Germany). The membranes were blocked with Protein-Free Rapid Sealing Solution (PS108P, Shanghai Epizyme Biomedical Technology Co., Ltd., Shanghai, China) for 30 min at room temperature, and followed by the following specific primary antibodies incubated overnight at 4 °C: anti-GAPDH (1:10,000, 10494-1-AP, Proteintech), anti-Activin A (1:500, ab89307, Abcam, Cambridge, UK), anti-ACVR2A (1:1000, ab134082, Abcam), anti-p-Smad2 (1:500, AF3449, Affinity Biosciences, Jiangsu, China), anti-p-Smad3 (1:500, AF3362, Affinity), anti-Smad2 (1:2000, 12570-1-AP, Proteintech), anti-Smad3 (1:500, AF6362, Affinity, or 1:500, PAC123Hu01, Cloud-Clone Corp), anti-LEF1 (1:1000, ab137872, Abcam), anti-Snail1 (1:500, 13099-1-AP, Proteintech), anti-TWIST (1:1000, 25465-1-AP, Proteintech), anti-ZEB1 (1:500, 21544-1-AP, Proteintech), anti- α -SMA (1:1000, ab137872, Abcam), anti-vimentin (1:2000, 10366-1-AP, Proteintech), and anti-VE-cadherin (1:1000, ab231227, Abcam, or 1:1000, ab33168, Abcam). The membranes were washed and then incubated with an HRP-coupled secondary antibody (1:10,000, ab97051, Abcam) for 1 h. An enhanced chemiluminescence (ECL) chemiluminescence kit (P2200, Suzhou New Saimei Biotechnology Co., Ltd., Suzhou, China) was used to visualize the final bands. The grayscale values of the bands corresponding to the final target protein were quantified via ImageJ software 1.53t (National Institutes of Health, Bethesda, MD, USA).

Table 1. Sequences of primers used in RT-qPCR.

Gene (rat)		5'–3'
α -Sma	Forward	GCGTGGCTATTCTTCGTGACTAC
	Reverse	CATCAGGCAGTTCGTAGCTCTTCTC
<i>Col1a1</i>	Forward	TGTTGGTCCTGCTGGCAAGAATG
	Reverse	GTCACCTTGTTTCGCTGTCTCAC
<i>Col3a1</i>	Forward	AGTCGGAGGAATGGGTGGCTATC
	Reverse	CAGGAGATCCAGGATGTCCAGAGG
<i>Ve-cadherin</i>	Forward	GATGCAGAGGCTCATGATGC
	Reverse	CTTGCGACTCACGCTTGACT
<i>Acrv2a</i>	Forward	CTTGCTCTTCAGGTGCTATACTTGG
	Reverse	GTCTGATTGGTTCTGTCTCTTTCCC
<i>Smad2</i>	Forward	GTCGTCCATCTTGCCATTCACTC
	Reverse	GTTCTCCACCACCTGCTCCTC
<i>Smad3</i>	Forward	AGGGCTTTGAGGCTGTCTACC
	Reverse	TGCTGGTCACTGTCTGTCTCC
<i>Lef-1</i>	Forward	CACACAACGGCATCCCTCATC
	Reverse	GGCTCCTGTTCCCTTCTCTGTTC
<i>Snail1</i>	Forward	CCGACCGCTCCAACCTACG
	Reverse	GCAGCCAGACTCTTGGTGTGTTG
<i>Twist</i>	Forward	TGAGCAACAGCGAGGAGGAG
	Reverse	CCGACTGCTGCGTCTCTTG
<i>Zeb1</i>	Forward	GCACAGCCAAGCACAGAAGAG
	Reverse	TGGAGAAGGTGGTTCAAGAGACTG
<i>Zeb2</i>	Forward	GAGATAAGGGAGAGCGTTGTG
	Reverse	AATGTGGTCTGGATCGTGG
β -actin	Forward	GGAGATTACTGCCCTGGCTCCTA
	Reverse	GACTCATCGTACTCCTGCTTGCTG
Gene (human)		5'–3'
<i>ACVR2A</i>	Forward	GGAAGTGGCTTCTCGTGTACTG
	Reverse	GCACAACAACCTTCTGCATGTCTTC
<i>SMAD2</i>	Forward	CGCCGCCAGTTGTGAAGAGAC
	Reverse	TCCTGCCCATCTGCTCTCCTC
<i>SMAD3</i>	Forward	GGAGCGGAGTACAGGAGACAGAC
	Reverse	CTAAGACACACTGGAACAGCGGATG
<i>LEF-1</i>	Forward	CACACAACGGCATCCCTCATCC
	Reverse	GCTCCTGCTCCTTTCTCTGTTTCATG
<i>SNAIL1</i>	Forward	CCTCGCTGCCAATGCTCATCTG
	Reverse	CTCTGCCACCCTGGGACTCTC
<i>TWIST</i>	Forward	GACTTCCTCTACCAGGTCTCCAG
	Reverse	TCCAGACCGAGAAGGCGTAGC
<i>ZEB1</i>	Forward	AGTGTTACCAGGGAGGAGCAGTG
	Reverse	TTTCTTGCCCTTCCTTCTGTGTC
<i>ZEB2</i>	Forward	TGACCTGCCACCTGGAACCTCC
	Reverse	GGCGGTACTTGATGTGCTCCTTC
<i>VE-CADHERIN</i>	Forward	GTACCACCTCACTGCTGTCTATTG
	Reverse	CAGGCACGGACGCATTGAAC
α -SMA	Forward	CTTCGTTACTACTGCTGAGC-GTGAG
	Reverse	CCCATCAGGCAACTCGTA-ACTCTTC
<i>VIMENTIN</i>	Forward	ATCGATGTGGATGTTTCCAA
	Reverse	TTGTACCATTCTTCTGCCTC

Table 1. Continued.

Gene (human)	5'–3'
GAPDH	Forward TGACATCAAGAAGGTGGTGAAGCAG
	Reverse GTGTCGCTGTTGAAGTCAGAGGAG

RT-qPCR, real-time quantitative polymerase chain reaction; α -SMA, α -smooth muscle actin; COL1A1, collagen type I alpha 1; COL3A1, collagen type III alpha 1; ACVR2A, activin receptor type IIA; LEF-1, lymphoid enhancer-binding factor 1; ZEB1, zinc Finger E-Box Binding Homeobox 1; ZEB2, zinc Finger E-Box Binding Homeobox 2; SNAIL1, snail family transcriptional repressor 1; TWIST, transcription factor twist family basic helix-loop-helix (bHLH) transcription factor 1; GAPDH, glyceraldehyde-3-phosphate dehydrogenase; SMAD, drosophila mothers against decapentaplegic.

2.12 Cell Scratch Assay

HUVECs were added to a 6-well plate. Once the HUVECs had adhered and proliferated, a pipette tip was used to gently make a wound in the central area of the cell layer. PBS was added for rinsing, and then, serum-free medium was added for culture. Images of the scratches were acquired with a phase contrast microscope at identical positions for 0 hours and 24 hours. The cell migratory capacity was assessed on the basis of the extent of healing observed in the scratched area.

2.13 Transwell Cell Migration Assay

HUVECs were transfected with ACVR2A-siRNA and treated with activin A. After they reached a sufficient treatment time, they were digested with trypsin. Then, 200 μ L of HUVECs were combined with serum-free medium and transferred to the upper chamber of a 24-well dish with an 8 μ m well. Additionally, 600 μ L of HUVECs mixed with 10% FBS medium was transferred to the bottom chamber. After a 12-hour incubation period, HUVECs were stabilized with 4% paraformaldehyde for 15 minutes and then stained with crystal violet solution (G1064, Solarbio) for 20 minutes. Images of HUVECs located on the underside of the luminal membrane were subsequently captured and quantitatively analyzed via an inverted microscope.

2.14 Statistical Analysis

GraphPad Prism 9.5 (GraphPad Software, San Diego, CA, USA) was used for statistical analysis of the data. The data are shown as the means \pm standard errors of the means. For comparisons of normally distributed data between two groups, an unpaired Student's *t*-test was used, whereas for pairwise comparisons among three or more groups, one-way ANOVA with Tukey's multiple comparisons test was used. In cases where the data were not normally distributed, a nonparametric test was employed. The data were considered statistically significant if the *p*-value was less than 0.05.

3. Results

3.1 AAV-siACVR2A Attenuates the Inflammatory Response and Fibrosis in RHD-Affected Valves

H&E staining revealed increased inflammatory infiltration in the mitral valvular tissues of rats in the RHD group. However, this inflammatory infiltration was reduced after the inhibition of ACVR2A (Fig. 1A). Sirius red staining was used to identify the collagen type, with type I collagen (COL1) appearing as tightly packed yellow and red fibers and type III collagen (COL3) appearing as loosely packed green fibers under a polarized light microscope. In nonfibrotic valves, COL1 is the primary collagen type, while the proportion of COL3 steadily increases as fibrosis progresses. As fibrosis progresses, the proportion of COL3 gradually increases, and an increase in the COL3/COL1 (COL3/1) ratio can be used to detect the onset of valvular fibrosis [42]. Our results revealed that the COL3/1 ratio was elevated in the RHD group. However, after inhibition of ACVR2A, the COL3/1 ratio decreased (Fig. 1B). The above results indicated that inflammatory infiltration and fibrotic changes occurred in the mitral valvular tissues of the rats in the RHD group, whereas the inflammatory infiltration and fibrosis of the valvular tissues were reduced after the inhibition of ACVR2A.

3.2 AAV-siACVR2A Inhibited Activin-Related Pathway-Mediated EndMT in RHD-Affected Valves

The immunohistochemistry results revealed that the expression of α -SMA, COL1A1, and vimentin was elevated in the valvular tissues of the RHD group. However, in the AAV-siACVR2A group, the above indices were decreased in the valvular tissues. In addition, CD31 was slightly reduced in the RHD group, but this slight reduction was reversed after the inhibition of ACVR2A (Fig. 2A). RT-qPCR analysis revealed that the mRNA levels of α -SMA, COL1A1, and COL3A1 were elevated in the valvular tissues of the RHD group. After pretreatment with AAV-siACVR2A, the levels of these indicators were reduced. In addition, the mRNA level of VE-cadherin, which is a characteristic indicator of endothelial cells, was decreased in the RHD group but recovered after the inhibition of ACVR2A (Fig. 2B). Western blotting analysis revealed that the protein expression of α -SMA and vimentin was increased in valvular tissues in the RHD group, whereas their expression was decreased in the AAV-siACVR2A group. In addition, the expression of VE-cadherin was decreased in the RHD group but recovered after the inhibition of ACVR2A (Fig. 2C). These results suggested that EndMT occurred in the valvular tissues of RHD rats and that inhibition of ACVR2A suppressed EndMT.

RT-qPCR analysis revealed that the mRNA levels of ACVR2A, LEF-1, Snail1, TWIST, ZEB1, and ZEB2 were significantly elevated in the RHD group, but these metrics decreased after the inhibition of ACVR2A. The mRNA expression of Smad2 and Smad3 did not significantly differ

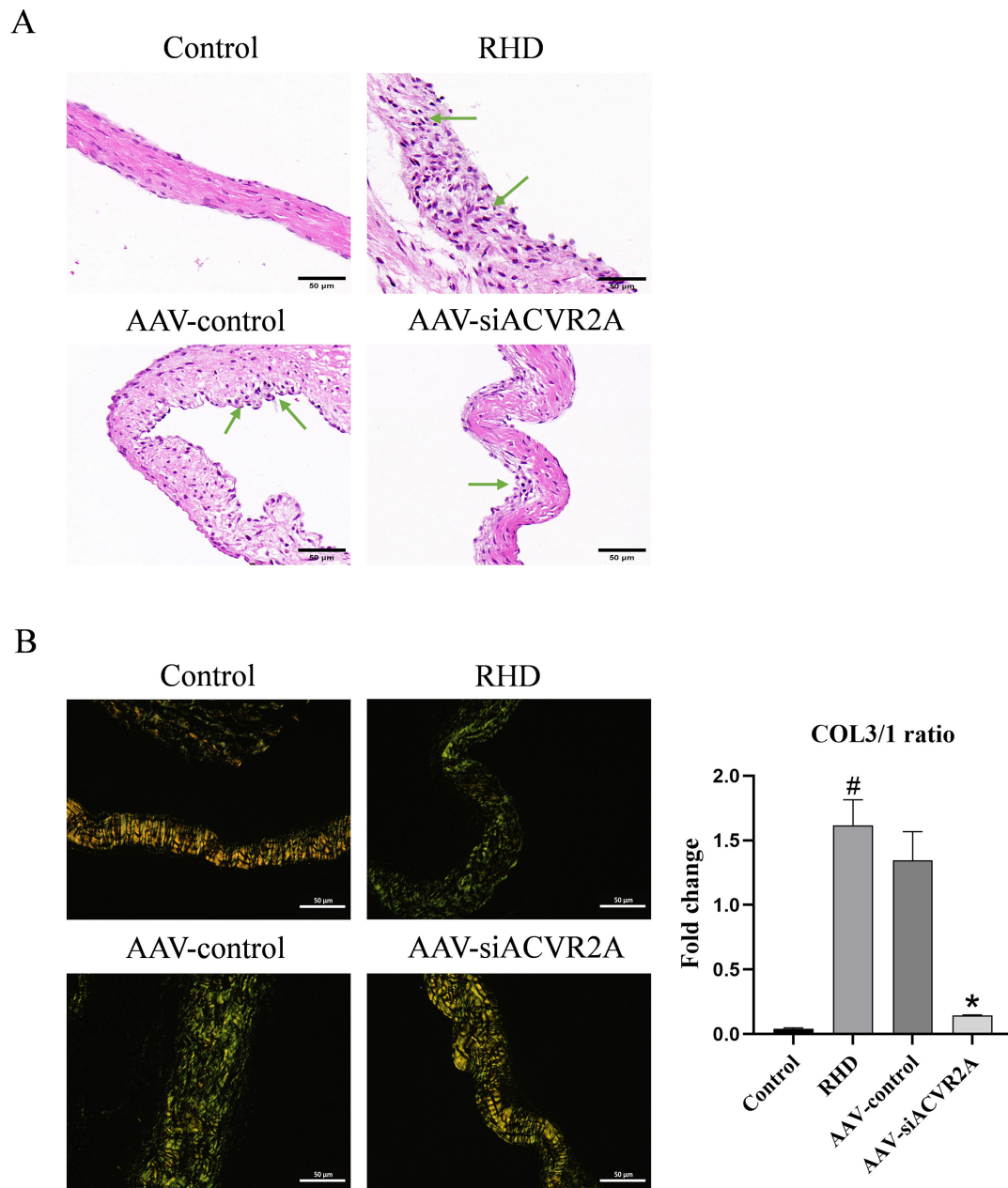


Fig. 1. AAV-siACVR2A attenuates the inflammatory response and fibrosis in RHD-affected valves. (A) H&E staining showing the severity of inflammatory cell infiltration in the mitral valvular tissues of the rats in each group. Magnification, $\times 400$. Scale bar = 50 μm . (B) Sirius red staining showing the degree of fibrosis in the mitral valvular tissues of the rats in each group (COL1 fibers are tightly arranged (yellow and red), and COL3 fibers are loosely arranged (green)) and the COL3/I ratio. Magnification, $\times 400$. Scale bar = 50 μm . # $p < 0.05$ compared with the control group. * $p < 0.05$ compared with the AAV-control group. $n = 6$. AAV, adeno-associated virus; RHD, rheumatic heart disease; H&E, hematoxylin and eosin; COL1, type I collagen; COL3, type III collagen.

between the groups (Fig. 2D). Western blotting analysis revealed that the protein expression of activin A, ACVR2A, p-Smad2, p-Smad3, Snail1, TWIST and ZEB1 was elevated in the RHD group, whereas these indices were reduced in the AAV-siACVR2A group. The protein expression of Smad2 and Smad3 did not differ significantly among the groups (Fig. 2E). The above results indicate that during EndMT in RHD valvular tissues, activin is activated, and

the expression of ACVR2A is subsequently elevated, which leads to the phosphorylation of Smad2/3 and then the activation of the intranuclear transcription factors involved in EndMT. In contrast, after the inhibition of ACVR2A, activin did not effectively phosphorylate Smad2/3, and related intranuclear transcription factors were not effectively activated, thus inhibiting EndMT in the valvular tissues of RHD rats.

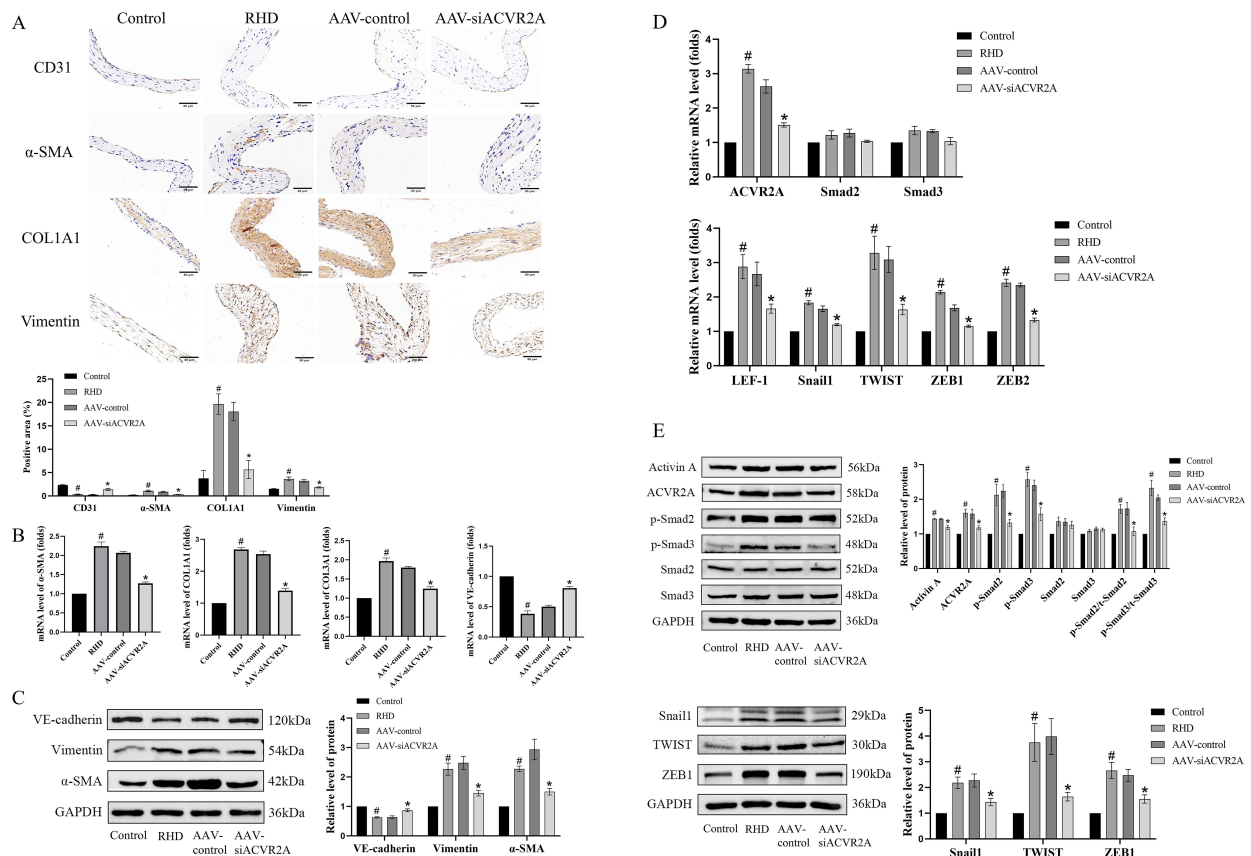


Fig. 2. AAV-siACVR2A inhibited activin-related pathway-mediated endothelial-mesenchymal transition (EndMT) in RHD-affected valves. (A) Immunohistochemical staining for CD31, α -SMA, COL1A1 and vimentin. Magnification, $\times 400$. Scale bar = 50 μ m. (B) RT-qPCR was used to measure the mRNA expression levels of α -SMA, COL1A1, COL3A1 and vascular endothelial (VE)-cadherin in rat valves. (C) Western blot analysis of the protein expression of VE-cadherin, vimentin and α -SMA in rat valves. (D) RT-qPCR analysis of the mRNA expression levels of factors related to the activin pathway in rat valves. (E) Western blot analysis of the protein expression of factors related to the activin pathway in rat valves. [#] $p < 0.05$ compared with the control group. ^{*} $p < 0.05$ compared with the AAV-control group. $n = 6$.

3.3 Activin A Promoted EndMT in HUVECs

RT-qPCR analysis revealed that the mRNA expression of ACVR2A, LEF-1, Snail1, TWIST, ZEB1, ZEB2, α -SMA, and vimentin was greater in the TGF- β 1 group and activin A group than in the control group, whereas the expression of VE-cadherin was lower in both groups. Smad2 and Smad3 mRNA expression did not differ significantly (Fig. 3A). Western blotting analysis revealed elevated protein expression of activin A, ACVR2A, p-Smad2, p-Smad3, LEF-1, Snail1, TWIST, ZEB1, α -SMA, and vimentin in the TGF- β 1 group and activin A group, whereas the expression of VE-cadherin was reduced in both groups. There was no significant difference in the protein expression of Smad2 and Smad3 (Fig. 3B). These results suggested that activation of activin A stimulated the mesenchymal transformation of HUVECs and that activin pathway-related factors were also activated during this process. The mesenchymal transformation of endothelial cells is closely related to the activation of activin and its signaling factors.

3.4 ACVR2A-siRNA Inhibited EndMT in HUVECs

RT-qPCR analysis revealed that the mRNA levels of ACVR2A, LEF-1, Snail1, TWIST, ZEB1, ZEB2, α -SMA, and vimentin were decreased in the ACVR2A-siRNA+activin A group and that the mRNA level of VE-cadherin was elevated in the ACVR2A-siRNA+activin A group compared with those in the NC-siRNA+activin A group. There was no significant difference in the mRNA expression of Smad2 and Smad3 (Fig. 4A). Western blotting analysis revealed that the protein expression of activin A, ACVR2A, p-Smad2, p-Smad3, Snail1, TWIST, ZEB1, α -SMA, and vimentin was reduced in the ACVR2A-siRNA+activin A group and that the protein expression of VE-cadherin tended to increase. There was no significant difference in the protein expression of Smad2 and Smad3 (Fig. 4B). In addition, the results of the scratch and Transwell migration assays revealed that migration was slower in the ACVR2A-siRNA+activin A group than in the NC-siRNA+activin A group (Fig. 4C,D). The above results indicated that after the inhibition of ACVR2A, the activa-

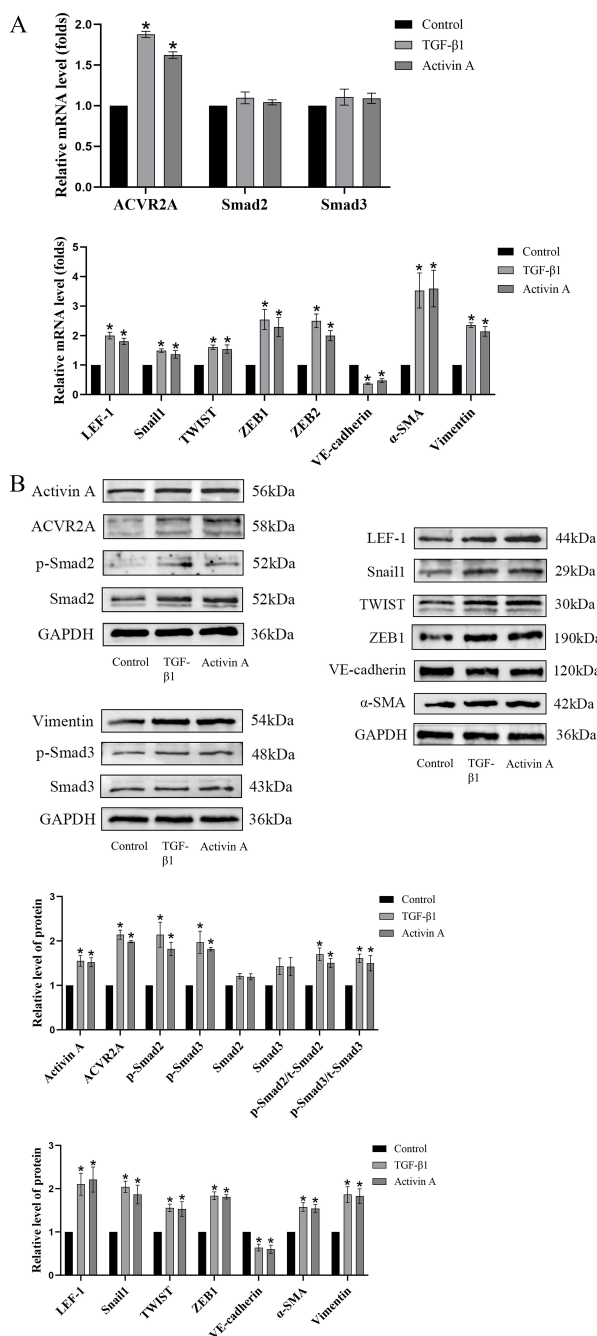


Fig. 3. Activin A promoted EndMT in human umbilical vein endothelial cells (HUVECs). (A) RT-qPCR was performed to measure the mRNA expression levels of activin pathway-related factors and EndMT-related factors in HUVECs during EndMT. (B) Western blot analysis of the protein expression of activin pathway-related factors and EndMT-related factors in HUVECs during EndMT. * $p < 0.05$ compared with the control group. $n = 3$. TGF, transforming growth factor.

tion of activin and its associated pathway factors was suppressed, and the mesenchymal transition of HUVECs was also inhibited. In addition, the motility of HUVECs during mesenchymal transformation was suppressed.

4. Discussion

EndMT is a complex biological process by which endothelial cells lose their endothelial phenotype and acquire a mesenchymal phenotype [10,11]. EndMT has been demonstrated to be involved in the development of the atrioventricular valve and is associated with the development of various inherited and acquired diseases, such as malignant, cardiovascular, inflammatory and fibrotic diseases. In the cardiovascular field, atherosclerosis, pulmonary hypertension, valvular heart disease and cardiac fibrosis are all associated with abnormal EndMT [43]. Notably, RHD is a disease that involves fibrotic changes in heart valves, and the role of EndMT in RHD valvular damage has recently been studied [32]. In our study, EndMT occurred in the valves of the RHD model rats. It is associated with mitral fibrosis.

The TGF- β signaling pathway is one of the major pathways regulating EndMT, and the key factors involved in this pathway include activin, Smad2, and Smad3 [16]. Activin belongs to the TGF- β superfamily of dimeric glycoproteins, in which the activin A subtype and TGF- β share the same signaling pathway at the Smad2/3/4 level [44]. Currently, activin and ACVR2A are receiving much attention in the study of antifibrosis and mesenchymal transition [34,35]. In skin tissues, activin is a potent regulator of wound repair and scar formation [45], and in acute mouse and human wounds, hyperproliferating keratinocytes in the wound epidermis as well as fibroblasts and inflammatory cells in granulation tissue were identified as sources of activin [46]. In liver fibrosis, activin was found to activate hepatic stellate cells, which led to increased expression of α -SMA and collagen, and exogenous follicular inhibitors eliminated the profibrotic effects of activin *in vitro*, which indicated that the inhibition of activin was effective in the treatment of liver fibrosis [47]. In addition, Liang J *et al.* [34] reported that echinacoside exerts potent antifibrotic effects by inhibiting the ACVR2A-mediated TGF- β 1/Smad signaling axis and could be used as an alternative therapy for hepatic fibrosis. In renal fibrosis, activin A promoted the proliferation of rat kidney fibroblasts, induced the expression of α -SMA and enhanced the mRNA expression of type I collagen, thereby exerting a profibrotic effect [48].

In our study, we revealed inflammatory infiltration and fibrotic changes in the valvular tissues of rats in the RHD disease model, and during the above pathology, the valvular tissues underwent EndMT, which was accompanied by the activation of activin and associated pathway factors. However, after inhibition of ACVR2A, activin pathway factor signaling was also suppressed, and mesenchymal indices were reduced, suggesting that EndMT in valvular tissues was suppressed and that inflammatory infiltration and fibrotic changes in valvular tissues were simultaneously reduced. In our *in vitro* study, activin A stimulated the mesenchymal transformation of endothelial cells, which was consistent with previous findings [49]. After inhibition

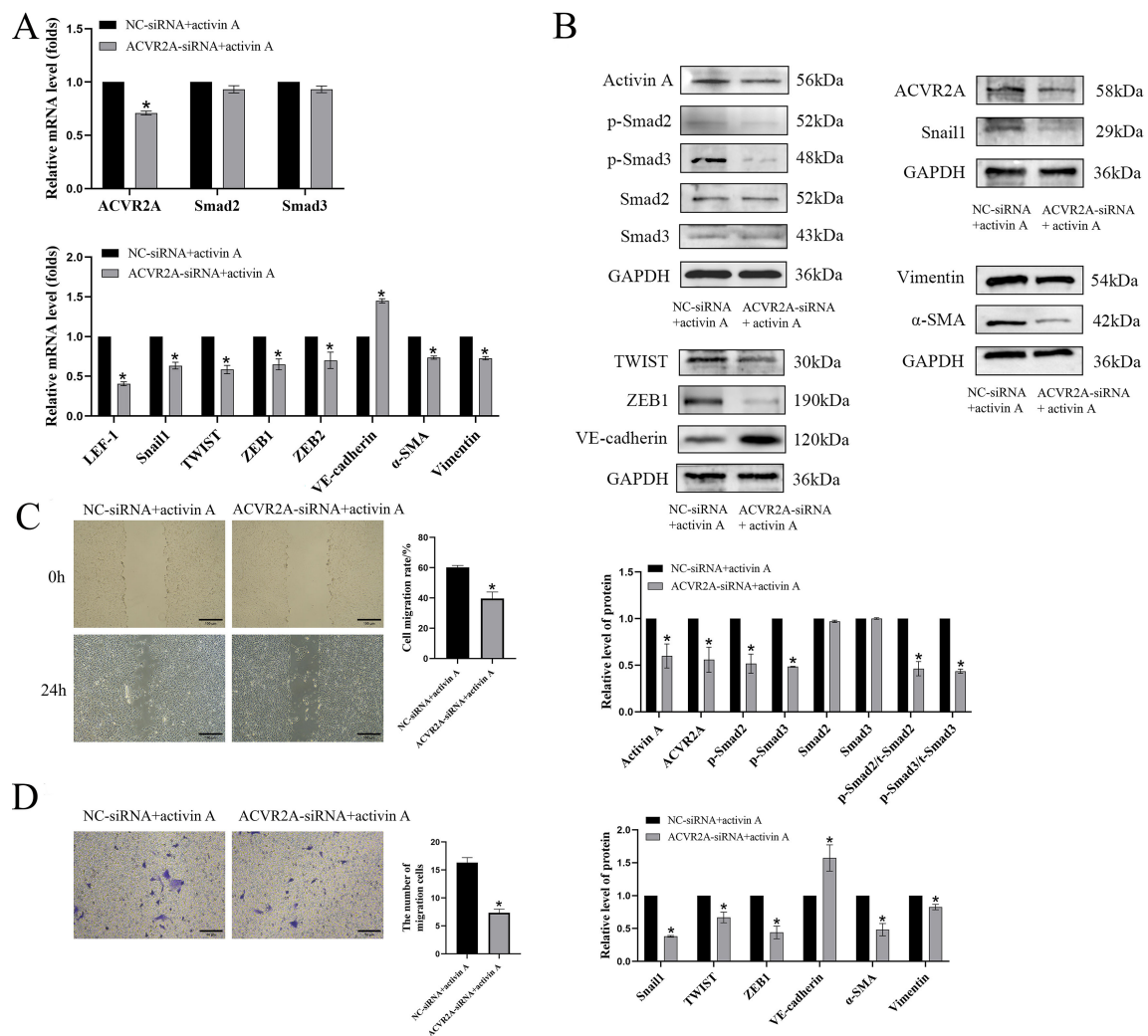


Fig. 4. ACVR2A-siRNA inhibited EndMT in HUVECs. (A) RT-qPCR analysis of the mRNA expression levels of activin pathway-related factors and EndMT-related factors in HUVECs after ACVR2A-siRNA treatment. (B) Western blot analysis of the protein expression of activin pathway-related factors and EndMT-related factors in HUVECs after ACVR2A-siRNA treatment. (C) Cell scratch assay using HUVECs. Magnification, $\times 40$. Scale bar = 100 μm . (D) Transwell migration assay using HUVECs. Magnification, $\times 200$. Scale bar = 50 μm . $*p < 0.05$ compared with the NC-siRNA+activin A group. $n = 3$.

of ACVR2A, mesenchymal transformation of endothelial cells was also inhibited. These results indicated that activin was activated by binding to ACVR2A, activated relevant intranuclear transcription factors via the Smad2/3 phosphorylation pathway, and caused mesenchymal transformation of endothelial cells, which, in turn, could lead to inflammatory infiltration and fibrotic changes in the valvular tissues of RHD rats. After inhibition of ACVR2A, there was a reduction in damage to valvular tissues. Because there is a relative paucity of treatments for RHD valvular injury, we believe that targeting ACVR2A may be a promising approach for the treatment of RHD valvular injury.

This study has several limitations. Firstly, we did not extract primary endothelial cells from the mitral valvular tissues of the RHD rat model, and further extraction of the primary valvular endothelium is needed for validation. Sec-

ondly, our conclusions were based on the RHD rat model, which does not accurately describe the pathomechanisms of human RHD valvulopathy accurately, and more subsequent combinatorial studies are needed to confirm these findings.

5. Conclusions

In conclusion, the present study demonstrated that inhibition of ACVR2A could mediate EndMT to attenuate valvular injury in RHD rats, further elucidating the mechanism of action of activin and EndMT in RHD valvular injury.

Availability of Data and Materials

The raw data supporting the conclusions of this article will be made available by the correspondence author (zengzhiyu@gxmu.edu.cn) on reasonable request.

Author Contributions

YZY, FH and CHL conceived and designed the study. ZRL and YL participated in the experimental design. ZRL and YL conducted the experiments. ZYM and LB analyzed the data. ZRL and YL drafted the manuscript. All authors contributed to editorial changes in the manuscript. All authors approved the final version. All authors agree to be accountable for all aspects of the work to ensure that questions related to the accuracy or integrity of any part of the work are appropriately investigated and resolved.

Ethics Approval and Consent to Participate

The protocol involving animals and patients has been approved by the Medical Ethics Committee of the First Affiliated Hospital of Guangxi Medical University (Approval Number: 202209145).

Acknowledgment

The authors would like to express their gratitude to American Journal Experts (<https://www.aje.cn>) for the expert linguistic services provided.

Funding

This work was supported by the National Natural Science Foundation of China (Grant No. 81960082), the Guangxi Key Laboratory of Precision Medicine in Cardio-cerebrovascular Diseases Control and Prevention (Grant No. 22-035-18), the Guangxi Clinical Research Center for Cardio-cerebrovascular Diseases (Grant No. AD17129014) and the Guangxi Medical High-level Backbone Talents “139” Program (Grant No. G201901006).

Conflict of Interest

The authors declare no conflict of interest.

References

- [1] Dooley LM, Ahmad TB, Pandey M, Good MF, Kotiw M. Rheumatic heart disease: A review of the current status of global research activity. *Autoimmunity Reviews*. 2021; 20: 102740. <https://doi.org/10.1016/j.autrev.2020.102740>.
- [2] Watkins DA, Johnson CO, Colquhoun SM, Karthikeyan G, Beaton A, Bukhman G, *et al.* Global, Regional, and National Burden of Rheumatic Heart Disease, 1990–2015. *The New England Journal of Medicine*. 2017; 377: 713–722. <https://doi.org/10.1056/NEJMoa1603693>.
- [3] Auala T, Zavale BG, Mbakwem AC, Mocumbi AO. Acute Rheumatic Fever and Rheumatic Heart Disease: Highlighting the Role of Group A Streptococcus in the Global Burden of Cardiovascular Disease. *Pathogens*. 2022; 11: 496. <https://doi.org/10.3390/pathogens11050496>.
- [4] Mirabel M, Narayanan K, Jouven X, Marijon E. Cardiology patient page. Prevention of acute rheumatic fever and rheumatic heart disease. *Circulation*. 2014; 130: e35–e37. <https://doi.org/10.1161/CIRCULATIONAHA.113.007855>.
- [5] Marijon E, Mirabel M, Celermajer DS, Jouven X. Rheumatic heart disease. *Lancet*. 2012; 379: 953–964. [https://doi.org/10.1016/S0140-6736\(11\)61171-9](https://doi.org/10.1016/S0140-6736(11)61171-9).
- [6] Marijon E, Mocumbi A, Narayanan K, Jouven X, Celermajer DS. Persisting burden and challenges of rheumatic heart disease. *European Heart Journal*. 2021; 42: 3338–3348. <https://doi.org/10.1093/eurheartj/ehab407>.
- [7] Salem A, Abdelgawad AME, Elshemy A. Early and Midterm Outcomes of Rheumatic Mitral Valve Repair. *The Heart Surgery Forum*. 2018; 21: E352–E358. <https://doi.org/10.1532/hsf.1978>.
- [8] Ngaage DL, Cowen ME, Griffin S, Guvendik L, Cale AR. Early neurological complications after coronary artery bypass grafting and valve surgery in octogenarians. *European Journal of Cardio-Thoracic Surgery*. 2008; 33: 653–659. <https://doi.org/10.1016/j.ejcts.2008.01.017>.
- [9] Passos LSA, Nunes MCP, Aikawa E. Rheumatic Heart Valve Disease Pathophysiology and Underlying Mechanisms. *Frontiers in Cardiovascular Medicine*. 2021; 7: 612716. <https://doi.org/10.3389/fcvm.2020.612716>.
- [10] Jiang Y, Zhou X, Hu R, Dai A. TGF- β 1-induced SMAD2/3/4 activation promotes RELM- β transcription to modulate the endothelium-mesenchymal transition in human endothelial cells. *The International Journal of Biochemistry & Cell Biology*. 2018; 105: 52–60. <https://doi.org/10.1016/j.biocel.2018.08.005>.
- [11] Peng Q, Shan D, Cui K, Li K, Zhu B, Wu H, *et al.* The Role of Endothelial-to-Mesenchymal Transition in Cardiovascular Disease. *Cells*. 2022; 11: 1834. <https://doi.org/10.3390/cells11111834>.
- [12] Xiong J, Kawagishi H, Yan Y, Liu J, Wells QS, Edmunds LR, *et al.* A Metabolic Basis for Endothelial-to-Mesenchymal Transition. *Molecular Cell*. 2018; 69: 689–698.e7. <https://doi.org/10.1016/j.molcel.2018.01.010>.
- [13] Li Y, Lui KO, Zhou B. Reassessing endothelial-to-mesenchymal transition in cardiovascular diseases. *Nature Reviews. Cardiology*. 2018; 15: 445–456. <https://doi.org/10.1038/s41569-018-0023-y>.
- [14] Bischoff J. Endothelial-to-Mesenchymal Transition. *Circulation Research*. 2019; 124: 1163–1165. <https://doi.org/10.1161/CIRCRESAHA.119.314813>.
- [15] Wu M, Lin J, Huang D, Ye C, Chen D. Salvianolic Acid C Inhibits the Epithelial-Mesenchymal Transition and Ameliorates Renal Tubulointerstitial Fibrosis. *Frontiers in Bioscience (Landmark Ed)*. 2023; 28: 121. <https://doi.org/10.31083/j.fbi2806121>.
- [16] Kovacic JC, Mercader N, Torres M, Boehm M, Fuster V. Epithelial-to-mesenchymal and endothelial-to-mesenchymal transition: from cardiovascular development to disease. *Circulation*. 2012; 125: 1795–1808. <https://doi.org/10.1161/CIRCULATIONAHA.111.040352>.
- [17] Gong L, Lei Y, Liu Y, Tan F, Li S, Wang X, *et al.* Vaccarin prevents ox-LDL-induced HUVEC EndMT, inflammation and apoptosis by suppressing ROS/p38 MAPK signaling. *American Journal of Translational Research*. 2019; 11: 2140–2154.
- [18] Piera-Velazquez S, Jimenez SA. Endothelial to Mesenchymal Transition: Role in Physiology and in the Pathogenesis of Human Diseases. *Physiological Reviews*. 2019; 99: 1281–1324. <https://doi.org/10.1152/physrev.00021.2018>.
- [19] Massagué J. How cells read TGF- β signals. *Nature Reviews. Molecular Cell Biology*. 2000; 1: 169–178. <https://doi.org/10.1038/35043051>.
- [20] Itoh S, Itoh F, Goumans MJ, Ten Dijke P. Signaling of transforming growth factor-beta family members through Smad proteins. *European Journal of Biochemistry*. 2000; 267: 6954–6967. <https://doi.org/10.1046/j.1432-1327.2000.01828.x>.
- [21] Moustakas A, Souchevsky S, Heldin CH. Smad regulation in TGF- β signal transduction. *Journal of Cell Science*. 2001; 114: 4359–4369. <https://doi.org/10.1242/jcs.114.24.4359>.
- [22] Pickup MW, Owens P, Moses HL. TGF- β , Bone Morphogenetic Protein, and Activin Signaling and the Tumor Microenvironment. *Cold Spring Harbor Perspectives in Biology*. 2017; 9: a022285. <https://doi.org/10.1101/cshperspect.a022285>.

- [23] Morianos I, Papadopoulou G, Semitekolou M, Xanthou G. Activin-A in the regulation of immunity in health and disease. *Journal of Autoimmunity*. 2019; 104: 102314. <https://doi.org/10.1016/j.jaut.2019.102314>.
- [24] Goh BC, Singhal V, Herrera AJ, Tomlinson RE, Kim S, Faugere MC, *et al.* Activin receptor type 2A (ACVR2A) functions directly in osteoblasts as a negative regulator of bone mass. *The Journal of Biological Chemistry*. 2017; 292: 13809–13822. <https://doi.org/10.1074/jbc.M117.782128>.
- [25] Thuault S, Tan EJ, Peinado H, Cano A, Heldin CH, Moustakas A. HMGA2 and Smads co-regulate SNAIL1 expression during induction of epithelial-to-mesenchymal transition. *The Journal of Biological Chemistry*. 2008; 283: 33437–33446. <https://doi.org/10.1074/jbc.M802016200>.
- [26] Vincent T, Neve EPA, Johnson JR, Kukalev A, Rojo F, Albanell J, *et al.* A SNAIL1-SMAD3/4 transcriptional repressor complex promotes TGF-beta mediated epithelial-mesenchymal transition. *Nature Cell Biology*. 2009; 11: 943–950. <https://doi.org/10.1038/ncb1905>.
- [27] Liu ZH, Zhang Y, Wang X, Fan XF, Zhang Y, Li X, *et al.* SIRT1 activation attenuates cardiac fibrosis by endothelial-to-mesenchymal transition. *Biomedicine & Pharmacotherapy*. 2019; 118: 109227. <https://doi.org/10.1016/j.biopha.2019.109227>.
- [28] Xu L, Fu M, Chen D, Han W, Ostrowski MC, Grossfeld P, *et al.* Endothelial-specific deletion of Ets-1 attenuates Angiotensin II-induced cardiac fibrosis via suppression of endothelial-to-mesenchymal transition. *BMB Reports*. 2019; 52: 595–600. <https://doi.org/10.5483/BMBRep.2019.52.10.206>.
- [29] Maleki S, Cottrill KA, Poujade FA, Bhattachariya A, Bergman O, Gâdin JR, *et al.* The mir-200 family regulates key pathogenic events in ascending aortas of individuals with bicuspid aortic valves. *Journal of Internal Medicine*. 2019; 285: 102–114. <https://doi.org/10.1111/joim.12833>.
- [30] Song S, Zhang R, Cao W, Fang G, Yu Y, Wan Y, *et al.* Foxm1 is a critical driver of TGF- β -induced EndMT in endothelial cells through Smad2/3 and binds to the Snail promoter. *Journal of Cellular Physiology*. 2019; 234: 9052–9064. <https://doi.org/10.1002/jcp.27583>.
- [31] Wang B, Wu Y, Ge Z, Zhang X, Yan Y, Xie Y. NLR5 deficiency ameliorates cardiac fibrosis in diabetic cardiomyopathy by regulating EndMT through Smad2/3 signaling pathway. *Biochemical and Biophysical Research Communications*. 2020; 528: 545–553. <https://doi.org/10.1016/j.bbrc.2020.05.151>.
- [32] Xian S, Chen A, Wu X, Lu C, Wu Y, Huang F, *et al.* Activation of activin/Smad2 and 3 signaling pathway and the potential involvement of endothelial mesenchymal transition in the valvular damage due to rheumatic heart disease. *Molecular Medicine Reports*. 2021; 23: 10. <https://doi.org/10.3892/mmr.2020.11648>.
- [33] Olsen OE, Wader KF, Hella H, Mylin AK, Turesson I, Nesthus I, *et al.* Activin A inhibits BMP-signaling by binding ACVR2A and ACVR2B. *Cell Communication and Signaling: CCS*. 2015; 13: 27. <https://doi.org/10.1186/s12964-015-0104-z>.
- [34] Liang J, Chen T, Xu H, Wang T, Gong Q, Li T, *et al.* Echinacoside Exerts Antihepatic Fibrosis Effects in High-Fat Mice Model by Modulating the ACVR2A-Smad Pathway. *Molecular Nutrition & Food Research*. 2024; 68: e2300553. <https://doi.org/10.1002/mnfr.202300553>.
- [35] Zhang H, Ruan Q, Chen C, Yu H, Guan S, Hu D, *et al.* Activin A/ACVR2A axis inhibits epithelial-to-mesenchymal transition in colon cancer by activating SMAD2. *Molecular Carcinogenesis*. 2023; 62: 1585–1598. <https://doi.org/10.1002/mc.23601>.
- [36] Chen A, Wen J, Lu C, Lin B, Xian S, Huang F, *et al.* Inhibition of miR 155 5p attenuates the valvular damage induced by rheumatic heart disease. *International Journal of Molecular Medicine*. 2020; 45: 429–440. <https://doi.org/10.3892/ijmm.2019.4420>.
- [37] Wen Y, Zeng Z, Gui C, Li L, Li W. Changes in the expression of Th17 cell-associated cytokines in the development of rheumatic heart disease. *Cardiovascular Pathology: the Official Journal of the Society for Cardiovascular Pathology*. 2015; 24: 382–387. <https://doi.org/10.1016/j.carpath.2015.07.006>.
- [38] Wu XD, Zeng ZY, Gong DP, Wen JL, Huang F. Potential involvement of S1PR1/STAT3 signaling pathway in cardiac valve damage due to rheumatic heart disease. *Biotechnic & Histochemistry: Official Publication of the Biological Stain Commission*. 2019; 94: 398–403. <https://doi.org/10.1080/10520295.2019.1574028>.
- [39] Chen X, Chen X, Shi X, Gao Z, Guo Z. Curcumin attenuates endothelial cell fibrosis through inhibiting endothelial-arterial transformation. *Clinical and Experimental Pharmacology & Physiology*. 2020; 47: 1182–1192. <https://doi.org/10.1111/1440-1681.13271>.
- [40] Jin YG, Yuan Y, Wu QQ, Zhang N, Fan D, Che Y, *et al.* Puerarin Protects against Cardiac Fibrosis Associated with the Inhibition of TGF- β 1/Smad2-Mediated Endothelial-to-Mesenchymal Transition. *PPAR Research*. 2017; 2017: 2647129. <https://doi.org/10.1155/2017/2647129>.
- [41] Zhu K, Cao C, Huang J, Cheng Z, Li D, Liu X, *et al.* Inhibitory effects of ursolic acid from Bushen Yijing Formula on TGF- β 1-induced human umbilical vein endothelial cell fibrosis via AKT/mTOR signaling and Snail gene. *Journal of Pharmacological Sciences*. 2019; 140: 33–42. <https://doi.org/10.1016/j.jphs.2019.04.001>.
- [42] Purushothaman KR, Purushothaman M, Turnbull IC, Adams DH, Anyanwu A, Krishnan P, *et al.* Association of altered collagen content and lysyl oxidase expression in degenerative mitral valve disease. *Cardiovascular Pathology*. 2017; 29: 11–18. <https://doi.org/10.1016/j.carpath.2017.04.001>.
- [43] Singh A, Bhatt KS, Nguyen HC, Frisbee JC, Singh KK. Endothelial-to-Mesenchymal Transition in Cardiovascular Pathophysiology. *International Journal of Molecular Sciences*. 2024; 25: 6180. <https://doi.org/10.3390/ijms25116180>.
- [44] Ge J, Sun H, Li J, Shan Y, Zhao Y, Liao F, *et al.* Involvement of CHOP in activin A induced myeloma NS 1 cell apoptosis. *Oncology Reports*. 2019; 42: 2644–2654. <https://doi.org/10.3892/or.2019.7382>.
- [45] Cruise BA, Xu P, Hall AK. Wounds increase activin in skin and a vasoactive neuropeptide in sensory ganglia. *Developmental Biology*. 2004; 271: 1–10. <https://doi.org/10.1016/j.ydbio.2004.04.003>.
- [46] Hübner G, Hu Q, Smola H, Werner S. Strong induction of activin expression after injury suggests an important role of activin in wound repair. *Developmental Biology*. 1996; 173: 490–498. <https://doi.org/10.1006/dbio.1996.0042>.
- [47] Wada W, Kuwano H, Hasegawa Y, Kojima I. The dependence of transforming growth factor-beta-induced collagen production on autocrine factor activin A in hepatic stellate cells. *Endocrinology*. 2004; 145: 2753–2759. <https://doi.org/10.1210/en.2003-1663>.
- [48] Yamashita S, Maeshima A, Kojima I, Nojima Y. Activin A is a potent activator of renal interstitial fibroblasts. *Journal of the American Society of Nephrology*. 2004; 15: 91–101. <https://doi.org/10.1097/01.asn.0000103225.68136.e6>.
- [49] Dean M, Davis DA, Burdette JE. Activin A stimulates migration of the fallopian tube epithelium, an origin of high-grade serous ovarian cancer, through non-canonical signaling. *Cancer Letters*. 2017; 391: 114–124. <https://doi.org/10.1016/j.canlet.2017.01.011>.